THEORETICAL AND APPLIED MECHANICS
Volume 50 (2023) Issue 2, 145–157 DOI: https://doi.org/10.2298/TAM231005008N

SECONDARY FLOWS OF PRANDTL'S SECOND KIND. MECHANISM OF FORMATION AND METHODS OF PREDICTION

Nikolay Nikitin

Abstract. In this paper a mechanism is formulated and a principle is proposed that makes it possible to explain and, in some cases, to predict the shape of secondary flows of Prandtl's second kind that arise in turbulent flows in straight pipes of non-circular cross-section. The effectiveness of the proposed principle is demonstrated by a number of known examples from the literature. The results of this work provide a rational basis for understanding the reasons for the formation and prediction of the shape of secondary flows of Prandtl's second kind in straight pipes of non-circular cross-section.

1. Introduction

Sometimes, a fluid flow that occurs under the influence of certain external factors causes, in turn, another flow, which in this case is called a *secondary flow*. Let's turn to some well-known examples.

The fluid in a straight pipe moves along the pipe, but when passing through a bend, a flow in the cross section also occurs (see Figure 1). This is called secondary flow. The cause of its occurrence is the force of inertia, which is often called centrifugal force. When moving along a curved trajectory, the centrifugal force acts outward, causing an increase in pressure on the outer wall of the pipe in the area of point B in Figure 1. Thus, there is a pressure gradient acting along the perimeter of the cross-section of the pipe, where the fluid velocity is zero and there are no inertia forces. The pressure gradient along the wall can only be balanced by the friction force acting against the motion, therefore, a secondary flow must occur, as shown in Figure 1.

Another example is the so-called Tea leaf paradox, described by Albert Einstein in 1926 [1]. When stirring tea in a round cup, the tea leaves at the bottom, contrary to expectations, gather in the center of the bottom, and not on the periphery (see Figure 2). The rotation speed of the water decreases with depth, hence the change

2020 *Mathematics Subject Classification:* 76F65; 76F40.
Key words and phrases: turbulent flows, secondary flows of Prandtl's 2nd kind, Navier-Stokes equations, direct numerical simulations.

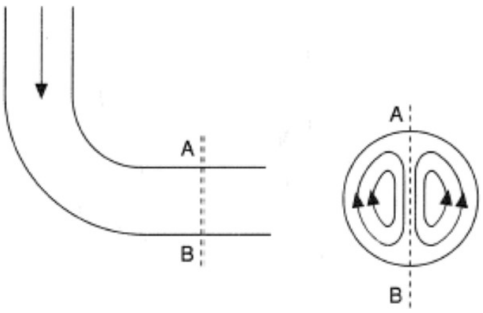

FIGURE 1. Occurrence of secondary flow in the bend of the pipe.

FIGURE 2. The tea leaf paradox.

in pressure on the wall caused by centrifugal force also decreases with depth. As a result, a meridional secondary flow occurs, in which water descends along the walls and rises in the central part of the cup.

In the considered examples, the cause of secondary flows is the centrifugal force that occurs when the fluid particles move along a curved trajectory. Such secondary flows are observed in both laminar and turbulent flows. They are usually called secondary flows of Prandtl's 1st kind, in contrast to secondary flows of the 2nd kind, which arise under the action of turbulent fluctuations.

2. Turbulent secondary flows in noncircular pipes

The most well-known secondary flows of Prandtl's 2nd kind are secondary flows in straight long pipes of non-circular cross-section. Nikuradze [2, 3] measured the mean velocity distributions over the cross-section of rectangular ducts and found that characteristic bulges appear in the corner regions in the turbulent flow (Figure 3).

L. Prandtl [4] suggested that such a specific distribution of the mean velocity is caused by the presence of secondary flows, the velocity of the fluid in which is directed towards the corners in the cross-sectional plane (Figure 4). The presence of secondary flows was confirmed in Nikuradse's later experiments [5]. The velocity

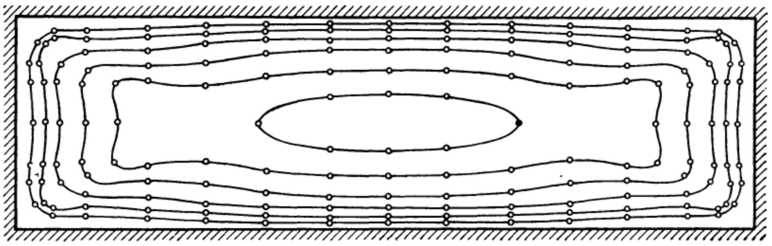

FIGURE 3. Distribution of mean velocity in turbulent flow in rectangular duct mesured by J. Nikuradse [3].

value in secondary flows in rectangular ducts was measured thirty years later [6]. It turned out that it did not exceed 1–2% of the mean flow rate. Nevertheless, as it was found later, secondary flows in turbulent flows make a significant contribution to the transverse transfer of mass, momentum, and heat.

The insignificant intensity complicates the experimental study of turbulent secondary flows. Since the 90s of the last century, significant progress has been made due to the development of methods for direct numerical simulation (DNS) of turbulent flows. In this approach, the turbulent flow is calculated with all the details by numerically solving the complete unsteady Navier–Stokes equations. An example of visualization of an instantaneous picture of turbulent flow in a pipe calculated by the author's method [7] is shown in Figure 5.

Mean flow characteristics are determined by statistical averaging of non-stationary fields. The average fields in long pipes do not change along the pipe. They only depend on the coordinates in the cross-section. The mean velocity field in the cross-section of a square duct is shown in Figure 6(a), [8]. Its characteristic feature is the bulges of the isolines in the corner regions. In accordance with Prandtl's assumption, in the vicinity of each of the corners, there is a secondary flow in the

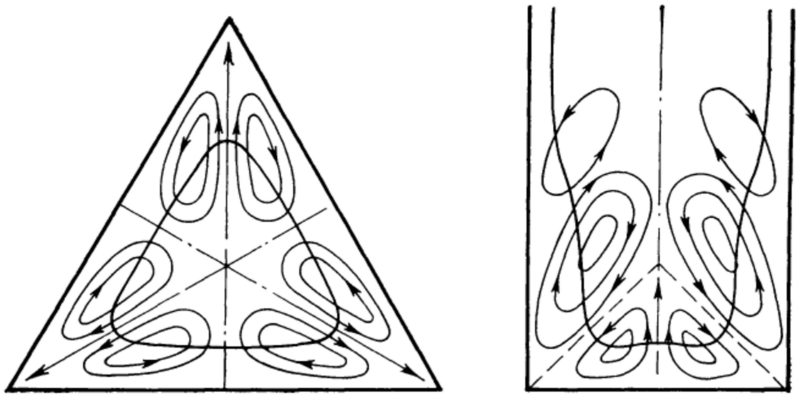

FIGURE 4. The scheme of secondary flows in turbulent flows in noncircular pipes proposed by L. Prandtl [4].

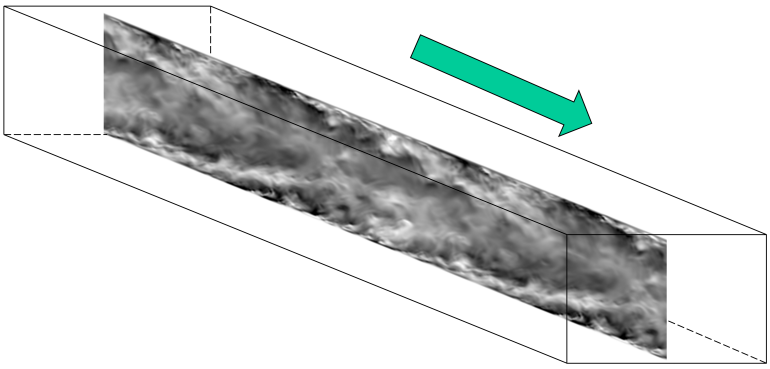

FIGURE 5. Instantaneous picture of turbulent flow in one of the longitudinal sections of the duct.

form of a pair of vortices of the opposite sign (Figure 6(b)), which carry high-velocity fluid particles from the outer flow to the corner regions. Here and in the following figures, solid streamlines correspond to the counterclockwise direction of fluid movement, and dashed lines correspond to clockwise movement.

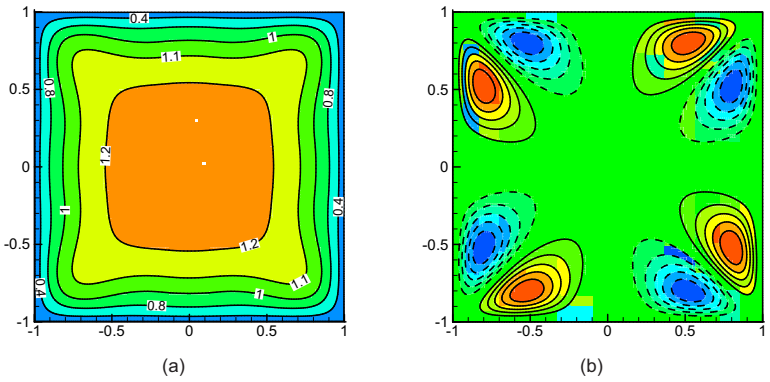

FIGURE 6. Turbulent flow in a square duct, [8]. (a) Mean velocity; (b) secondary flow.

Secondary flows in the vicinity of the outer corner (Figure 7) have the opposite direction [8, 9]. Fluid particles move along the bisector from the corner towards the outer flow. Accordingly, the bulges of the mean velocity isolines are directed out from the corner, and not towards the corner, as in the vicinity of the inner corners.

3. Mechanism of secondary flow formation

The distributions of the mean quantities in a turbulent flow are described by the Reynolds equations. The equations for the cross-stream mean velocities V and

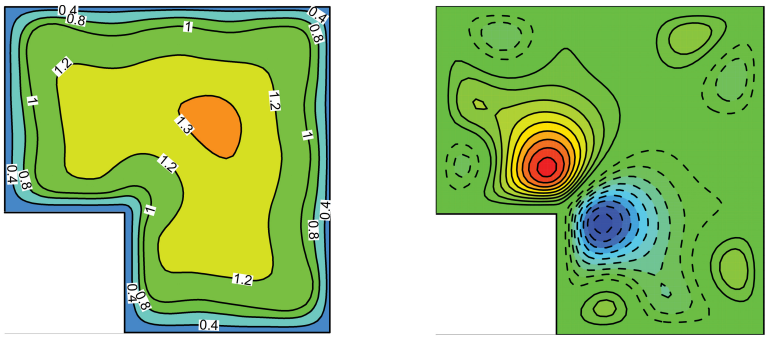

FIGURE 7. Turbulent flow along an outer corner, [8]. (a) Mean velocity; (b) secondary flow.

W read

$$V\frac{\partial V}{\partial y}+W\frac{\partial V}{\partial z}-\nu\Big(\frac{\partial^2 V}{\partial y^2}+\frac{\partial^2 V}{\partial z^2}\Big)+\frac{\partial P}{\partial y}=-\frac{\partial\overline{v'v'}}{\partial y}-\frac{\partial\overline{v'w'}}{\partial z}$$

$$V\frac{\partial W}{\partial y}+W\frac{\partial W}{\partial z}-\nu\Big(\frac{\partial^2 W}{\partial y^2}+\frac{\partial^2 W}{\partial z^2}\Big)+\frac{\partial P}{\partial z}=-\frac{\partial\overline{v'w'}}{\partial y}-\frac{\partial\overline{w'w'}}{\partial z}$$

$$\frac{\partial V}{\partial y}+\frac{\partial W}{\partial z}=0$$

We assume that the flow is statistically homogeneous in the direction of the flow; therefore, all derivatives with respect to longitudinal coordinate x are set to zero. In the last equations ν is fluid viscosity, P denotes mean pressure, v' and w' denote turbulent velocity fluctuations and overbar denotes averaging.

The presence of a secondary flow is characterized by the longitudinal component $\Omega_x=\partial W/\partial y-\partial V/\partial z$ in the mean vorticity vector. The equation for Ω_x reads [10]

$$V\frac{\partial\Omega_x}{\partial y}+W\frac{\partial\Omega_x}{\partial z}-\nu\Big(\frac{\partial^2\Omega_x}{\partial y^2}+\frac{\partial^2\Omega_x}{\partial z^2}\Big)=S$$

On the left-hand side, it contains convective and viscous terms, and on the right-hand side, there is source term S, which is expressed in terms of the Reynolds stress gradients:

$$S=\frac{\partial^2}{\partial y\partial z}(\overline{v'^2}-\overline{w'^2})+\Big(\frac{\partial^2}{\partial z^2}-\frac{\partial^2}{\partial y^2}\Big)\overline{v'w'}\equiv S_1+S_2$$

In the absence of turbulent fluctuations, the source S is equal to zero, and there is no secondary flow. Thus turbulent fluctuations are the only reason for the appearance of secondary flows in straight long channels.

In a large number of papers, attempts are made to explain the mechanism of occurrence of secondary flows and to predict their shape based on an analysis of the distributions of the S_1 and S_2 terms expressed in terms of the normal and shear Reynolds stresses [10–19]. Attempts are made to give these terms a definite physical meaning. In our opinion, such approaches are unpromising, since the quantities

S_1 and S_2 are not invariants. Their values change when the y, z coordinate system is rotated. In particular, the values of S_1 and S_2 are reversed when the coordinate axes are rotated by 45 degrees [11].

Physical mechanism of the occurrence of secondary flows in turbulent flows along the corners can be explained in the following simple way [8, 20]. Let us first turn to the case of motion along an inner corner. In turbulent flows along a flat wall, velocity fluctuations in the near-wall region predominantly occur along the wall, since the transverse motions are restricted by the wall. Thus, the trajectories of the fluid particles in the corner region, connecting two flat sections in the projection onto the plane perpendicular to the flow, have a curvilinear shape with a convexity directed towards the corner (Figure 8). The resulting centrifugal force is balanced by a pressure gradient, which means an increase in pressure in the corner area. There are no fluctuations on solid walls; therefore, the effect of the pressure gradient force along the walls can be neutralized only by the friction force directed against the movement of the fluid. Thus, the fluid spreads along the walls in both directions from the corner, which is compensated by the fluid flowing to the corner from the outer flow along the bisector. The well-known picture of the secondary flow arises.

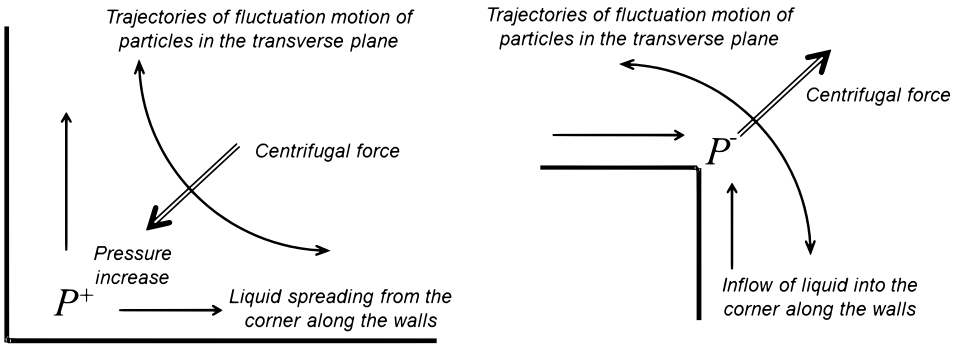

FIGURE 8. Physical mechanism of the occurrence of turbulent secondary flows in the vicinity of the inner and outer corners, [8].

In the flow along the outer corner, the opposite picture arises. The trajectories of fluctuations are convexly directed away from the corner, which leads to a pressure decrease in the corner region, fluid inflow along the walls, and movement towards the outer flow along the bisector.

4. Prediction of secondary flows

The consideration that the fluid in the secondary flow moves along the walls from higher pressure to lower pressure leads to the conclusion that the points of local extrema of the mean pressure on the wall are critical points of the streamlines of the secondary flow. The shape of the secondary flows in the vicinity of the local minimum and maximum pressure on the wall is shown in Figure 9. This can be used to predict the shape of secondary flows in pipes of arbitrary non-circular cross-section. If we can determine the location of local mean pressure extrema along the

perimeter of the cross-section of the pipe, we can largely predict the shape of the emerging secondary flows.

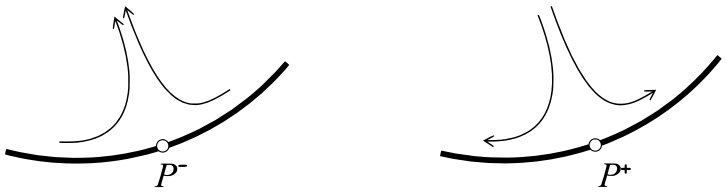

FIGURE 9. Secondary flow streamlines in the vicinity of the wall pressure local minimum P^- and maximum P^+, [8, 20].

The distribution of the mean pressure along the wall is related to the curvature of the wall. Consider three options for the curvature of the wall: concave, flat, and convex. Let us direct the y-axis along the normal, and the z-axis along the tangent to the wall at the selected point (Figure 10). In the absence of secondary flow, the relationship between the pressure gradient in y direction and the Reynolds stress gradients may be written as

$$-\frac{\partial(P+\overline{v'^2})}{\partial y} = \frac{\partial \overline{v'w'}}{\partial z}.$$

If the right-side term is positive, then the sum $P+\overline{v'^2}$ increases approaching the wall. It means that pressure increase on the wall since v' is equal to zero here. In the vicinity of the wall, the velocity fluctuations are directed along the wall; therefore, at the concave wall, the production $v'w'$ is mainly negative at left and positive at the right of the considered point (Figure 10(a)). Thus, the right-side term is positive, which corresponds to wall-pressure increase. This is marked by P^+ in the figure. In the vicinity of the convex wall, shown in Figure 10(c), on the contrary, the right-side term is negative which leads to a decrease in pressure. At a flat wall, the action of the right-side term is neutral.

It can be assumed that when the curvature of the wall changes along the perimeter, a proportional change in the mean pressure can be expected. Thus, mean pressure extrema at the cross-sectional boundary should be expected at the points of curvature extrema.

The formulated considerations can be used to predict the shape of secondary flows for pipes of different cross-sections. To do this, one should try to find the points of local pressure extrema along the perimeter of the cross-section based on the curvature of the boundary, symmetry conditions, and maybe some other considerations. Let us look at some examples. Figure 11 shows the results of direct numerical simulation of turbulent flow in a pipe with a triangle-like cross-section. In the cross-section, there are three inner corners A, B, B', in which, for obvious reasons, local pressure maxima are achieved. Between them, at some intermediate points of the lateral boundaries C and C', as well as in the middle of the lower boundary D, local pressure minima are expected. All this is confirmed by the DNS

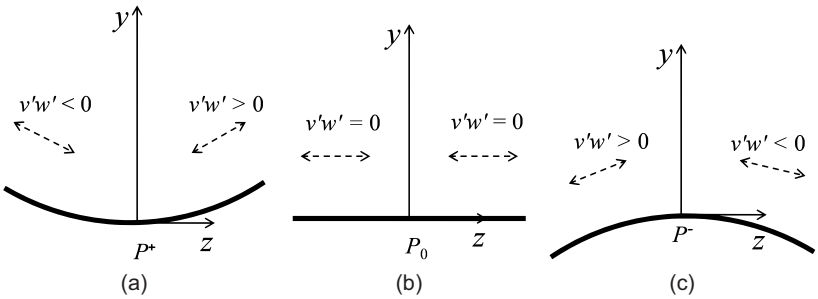

FIGURE 10. The relationship of the $v'w'$ to the curvature of the boundary, [8, 20].

results. The shape of the secondary flows qualitatively corresponds to the location of the local pressure extrema.

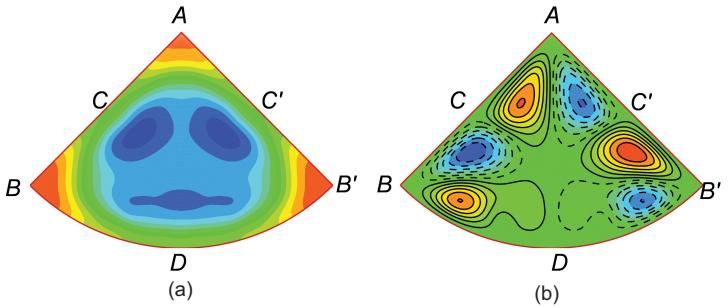

FIGURE 11. (a) Mean pressure; and (b) secondary flow in a pipe with triangle-like cross-section, [8, 20].

The next example, presented in Figure 12, shows results for the circular cross-section with a deleted sector. In such a section, there are two inner corners with pressure maxima and one outer corner where a local pressure minimum is reached. Note that the change in pressure, in this case, is considered only along the perimeter of the cross-section of the pipe. Therefore, a decrease in pressure in the vicinity of point A inside the flow area is not a contradiction. The pressure change along the CC' arc is less predictable in this case. The flow at the point of symmetry D is largely determined by the motion in the vicinity of corner A; therefore, at point D, one should rather expect a local maximum of pressure than a local minimum. If so, then the local minima should be somewhere in the intermediate points B and B'. Drawing streamlines of the secondary motion in the vicinity of local extrema of the wall pressure in accordance with the types of these extrema, we obtain a picture of the secondary motion, topologically equivalent to what is obtained in the numerical simulation. If we assume the presence of a local pressure minimum at point D, then a different picture will turn out, which is not realized in this case but is possible, for example, with a different value of the angle at the vertex A.

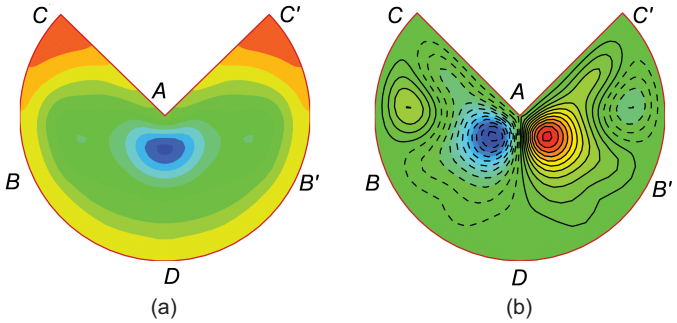

FIGURE 12. (a) Mean pressure; and (b) secondary flow in a circular pipe with deleted sector, [8, 20].

Let us consider a few more cases known from the literature, shown in Figure 13. In an elliptical pipe (Figure 13(a)), the points of maximum curvature of the boundary are reached at the ends of the major diameter. In these points, a local pressure maximum is achieved, and the streamlines of the secondary flow diverge from these points along the wall. Conversely, a minimum of pressure is achieved at the ends of the smaller diameter. Fluid flows to these points along the wall. Predicted results correspond to results of DNS [19, 21]. In a rectangular pipe with rounded corners [22] (Figure 13(b)), the situation is similar to the case of non-rounded walls. The maximum pressure arises at the points of maximum curvature of the boundary in the corner regions, and the shape of the secondary vortices does not change qualitatively. The rearrangement occurs when the flat area with a minimum pressure at the lower boundary disappears completely (Figure 13(c)). In this case, the picture of the secondary flow from a four-vortex one turns into a two-vortex one [23].

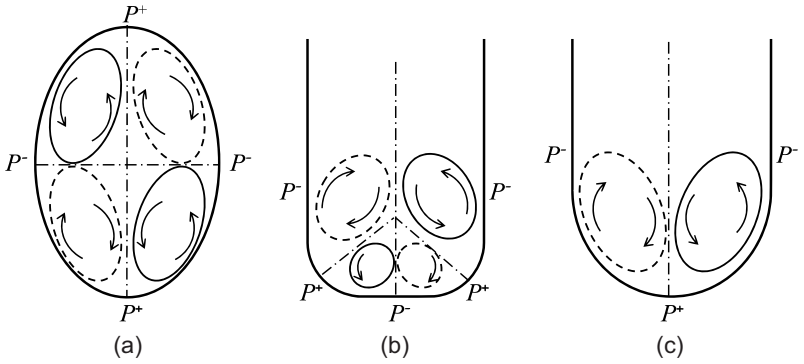

FIGURE 13. Schemes of secondary flows in pipes of various cross-sections, [8, 20].

Does the proposed principle predict secondary flows in all cases? Of course not. The simplest example is a pipe with an eccentric annular cross-section [24, 25]. The

curvature of both walls in this pipe is constant along the perimeter, which does not give the opportunity to determine the points of pressure extrema. However, the Reynolds stresses change along the perimeter and secondary flows arise.

5. Flow in an open channel

Secondary flows are of great importance in open channels. There are many papers on this subject. The generally accepted picture of secondary flows in channels with a free boundary, [26] is schematically depicted in Figure 14. In the area of the lower corner between the solid walls, we have the usual picture with two vortices and divergent flows along the walls. And in the corner where the solid and free walls meet, there is movement directed upwards along the solid wall. Using the above considerations, we can immediately say that such a scheme is erroneous. It is obvious, that there must be an increased pressure in the upper corner, which means that along the vertical wall, where the no-slip conditions are met, the fluid must fall down, and not rise up.

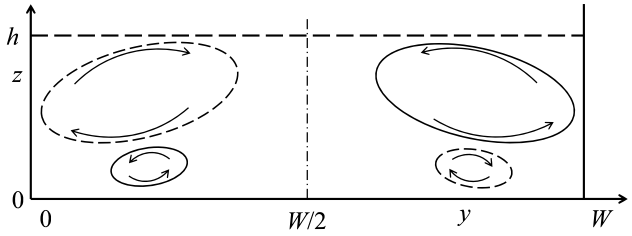

FIGURE 14. Scheme of secondary flow in an open channel, [20].

The results of direct numerical simulation [8, 20], shown in Figure 15 confirm the predictions. On the whole, the picture of the secondary flow corresponds to the accepted scheme, however, near the upper corners there are small single vortices that ensure the lowering of the fluid along the vertical walls. The calculations are carried out in the approximation of a flat free surface, so the pressure is not constant along the upper boundary. There exist an experimental confirmation of the described picture [27].

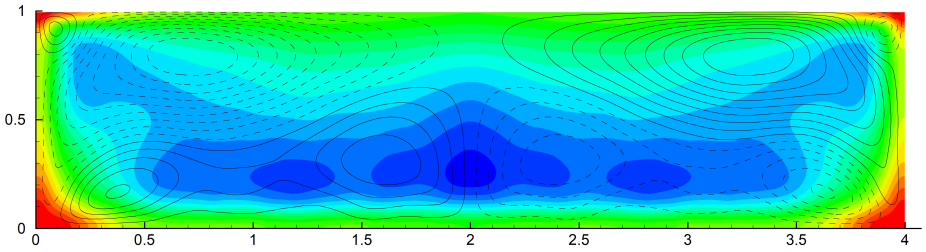

FIGURE 15. Mean pressure and secondary flow in an open channel, [8, 20].

6. Conclusion

The mechanism and a simple principle is formulated in this paper, which makes it possible to explain and, in some cases, to predict the shape of secondary flows of Prandtl's second kind that arise in turbulent flows in straight pipes of non-circular cross-section. The secondary flows are consistent with the distribution of the mean pressure along the cross-sectional boundary. Fluid moves along the boundary from high to low mean pressure, since there are no Reynolds stress forces on the no-slip solid wall, and the pressure force can be balanced only by the viscous friction force acting opposite to the motion direction. Thus, the direction of secondary motion along the pipe perimeter can be determined by the location of the local mean wall pressure extrema. In some cases, the location of local pressure extrema can be established based on the analysis of the wall curvature. The greater the curvature of the wall, the greater the change in pressure occurs under the influence of velocity fluctuations. On the convex boundary, an increase in pressure occurs, while on the concave, on the contrary, a decrease occurs. The effectiveness of the proposed principle is demonstrated by a number of examples, such as the flows in a square duct, in an elliptical pipe, in pipes with a section in the form of a circular sector with an apex angle of 90° and 270°, in rectangular ducts with rounded corners, in an eccentric annular tube. In most cases, the approximate picture of secondary flows can be predicted a priori using only symmetry considerations and an analysis of the curvature of the cross-sectional boundary.

The results of this paper provide a rational basis for understanding the reasons for the formation and prediction of the shape of secondary flows of Prandtl's second kind in straight pipes of non-circular cross-section.

Acknowledgments. The reported study was funded by RSF, project number 22-21-00184. The research was carried out using the computing resources of the federal collective usage center Complex for Simulation and Data Processing for Mega-science Facilities at NRC "Kurchatov Institute" (ministry subvention under agreement RFMEFI62117X0016).

References

1. A. Einstein, *Ursache der Meanderbildung der Flusslaufe und des sogenannten Baerschen Gesetzes*, Die Naturwissenschaften **14**(11) (1926), 223–224.
2. J. Nikuradse, *Untersuchung über die Geschwindigkeitsverteilung in turbulenten Strömungen*, V.D.I. Forschungsheft **70** (1926), 1229–1230.
3. H. Schlichting, *Grenzschicht-Theorie*, Verlag G. Braun, Karlsruhe, 1965.
4. L. Prandtl, *Über die ausgebildete Turbulenz*, 2nd Intl Kong. für Tech. Mech., Zürich, 1926.
5. J. Nikuradse, *Turbulente strömung in nicht-kreisförmigen rohren*, Ing.-Arch. **1** (1930), 306–332.
6. L. C. Hoagland, *Fully developed turbulent flow in straight rectangular ducts — secondary flow, its cause and effect on the primary flow*, PhD thesis, Department of Mechanical Engineering, Massachusetts Institute of Technology, 1960.
7. N. Nikitin, *Finite-difference method for incompressible Navier-Stokes equations in arbitrary orthogonal curvilinear coordinates*, J. Comput. Phys. **217**(2) (2006), 759-781.
8. N. V. Nikitin, N. V. Popelenskaya, A. Stroh *Prandtl's secondary flows of the second kind. Problems of description, prediction, and simulation*, Fluid Dyn. **56**(4) (2021), 513–538.

9. N. Nikitin, B. Krasnopolsky *Turbulent flows along a streamwise external corner*, J. Fluid Mech. **940** (2022), A16.
10. H. A. Einstein, H. Li *Secondary currents in straight channels*, Trans. Am. Geophys. Union. **39**(6) (1958), 1085–1088.
11. E. Brundrett, W. D. Baines *The production and diffusion of vorticity in duct flow*, J. Fluid Mech. **19**(3) (1964), 375–394.
12. F. B. Gessner, J. B. Jones *On some aspects of fully-developed turbulent flow in rectangular channels*, J. Fluid Mech. **23**(4) (1965), 689–713.
13. H. J. Perkins *The formation of streamwise vorticity in turbulent flow*, J. Fluid Mech. **44** (1970), 721–740.
14. C. G. Speziale *On turbulent secondary flows in pipes of noncircular cross-section*, Intl J. Engng Sci. **20**(7) (1982), 863–872.
15. A. O. Demuren, W. Rodi *Calculation of turbulence-driven secondary motion in non-circular ducts*, J. Fluid Mech. **140** (1984), 189–222.
16. S. Gavrilakis *Numerical simulation of low-Reynolds-number turbulent flow through a straight square duct*, J. Fluid Mech. **244** (1992), 101–129.
17. A. Huser, S. Biringen *Direct numerical simulation of turbulent flow in a square duct*, J. Fluid Mech. **257** (1993), 65–95.
18. H. Xu, A. Pollard *Large eddy simulation of turbulent flow in a square annular duct*, Phys. Fluids **13**(11) (2001), 3321–3337.
19. T. V. Voronova, N. V. Nikitin *Results of direct numerical simulation of turbulent flow in a pipe of elliptical cross-section*, Fluid Dyn. **42**(2) (2007), 201–211.
20. N. Nikitin *Turbulent secondary flows in channels with no-slip and shear-free boundaries*, J. Fluid Mech. **917** (2021), A24.
21. N. Nikitin, A. Yakhot *Direct numerical simulation of turbulent flow in elliptical ducts*, J. Fluid Mech. **532** (2005), 141–164.
22. A. Vidal, R. Vinuesa, P. Schlatter, H. M. Nagib *Impact of corner geometry on the secondary flow in turbulent ducts*, in: Proceedings of the 10^{th} International Symposium on Turbulence and Shear Flow Phenomena, *TSFP-10*, Chicago, USA, 2017.
23. A. Vidal, R. Vinuesa, P. Schlatter, H. M. Nagib *Turbulent rectangular ducts with minimum secondary flow*, Int. J. Heat Fluid Flow **72** (2018), 317–328.
24. N. V. Nikitin *Direct simulation of turbulent flow in eccentric pipes*, Comp. Maths Math. Phys. **46**(3) (2006), 489–504.
25. N. Nikitin, H. Wang, S. Chernyshenko *Turbulent flow and heat transfer in eccentric annulus*, J. Fluid Mech. **638** (2009), 95–116.
26. I. Nezu, H. Nakagawa *Turbulence in Open-Channel Flows*, Monograph of IAHR; Balkema: Rotterdam, The Netherlands, 1993.
27. L. M. Grega, T. Wey, R. I. Leighton, J. C. Neves *Turbulent mixed-boundary flow in a corner formed by a solid wall and a free-surface*, J. Fluid Mech. **294** (1995), 17–46.

СЕКУНДАРНИ ТОКОВИ ПРАНДТЛОВЕ ДРУГЕ ВРСТЕ. МЕХАНИЗАМ НАСТАНКА И МЕТОДЕ ПРЕДВИЂАЊА

Резиме. Формулисан је механизам и предложен принцип који омогућава објашњење, а у неким случајевима и предвиђање облика секундарних струјања Прандтлове друге врсте која настају у турбулентним струјањима у равним цевима некружног пресека. Ефикасност предложеног принципа показује низ познатих примера из литературе. Резултати овог рада дају рационалну основу за разумевање разлога за настанак и предвиђање облика секундарних токова Прандтлове друге врсте у равним цевима некружног пресека.

Institute of Mechanics
Lomonosov Moscow State University
Moscow
Russia
nvnikitin@mail.ru

(Received 05.10.2023)
(Revised 25.10.2023)
(Available online 10.11.2023)